Geophysical Research Letters

RESEARCH LETTER
10.1029/2024GL111276

Iron Content-Dependence of Ferropericlase Elastic Properties Across the Spin Crossover From Novel Experiments and Machine Learning

V. E. Trautner[1], A. Rijal[2], C. Plueckthun[3], N. Satta[1,4], E. Koemets[1,5], J. Buchen[1,6], B. Wang[1], K. Glazyrin[3], L. Cobden[2], and H. Marquardt[1]

[1]Department of Earth Sciences, University of Oxford, Oxford, UK, [2]Department of Earth Sciences, Utrecht University, Utrecht, The Netherlands, [3]Deutsches Elektronen-Synchrotron DESY, Hamburg, Germany, [4]Now at Institut für Mineralogie, Universität Münster, Münster, Germany, [5]Now at Diamond Light Source Ltd, Harwell Science and Innovation Campus, Didcot, UK, [6]Now at Bayerisches Geoinstitut, University of Bayreuth, Bayreuth, Germany

Abstract The iron spin crossover in $(Mg_{1-x}Fe_x)O$ ferropericlase causes changes to its physical properties that are expected to affect seismic velocities in Earth's lower mantle. We present new time-resolved pressure-volume measurements of iron-rich ferropericlase ($x_{Fe} = 0.40, 0.59$) and combine the results with literature data with $x_{Fe} = 0.04$–0.6 to investigate the dependence of ferropericlase elastic properties on iron content. We infer the relationship between unit-cell volume, pressure and iron content directly from the data by training Mixture Density Networks and derive bulk modulus, density and bulk sound velocity from the outputs. This allows us to constrain the effect of the spin crossover on these properties and estimate their uncertainties for different iron contents. Our findings indicate that the spin crossover may significantly alter the physical properties of ferropericlase in iron-enriched regions in the lowermost mantle, with implications for the interpretation of seismic heterogeneities observed near the core-mantle boundary.

Plain Language Summary The most voluminous layer in Earth's interior is the lower mantle, the deepest layer above the core. About 18% consists of the mineral ferropericlase, an iron-magnesium oxide. Under the extreme pressures in the lower mantle, the iron atoms of ferropericlase change at the electronic level, in a process called the spin crossover. This leads to changes in the material properties of ferropericlase that affect seismic wave speeds. Seismic waves are produced by earthquakes and can be used to investigate Earth's interior, but interpreting seismic observations requires constraints on the properties of mantle minerals. Here we investigate how the spin crossover depends on ferropericlase iron content. We conducted new high-pressure experiments on samples containing 40% and 59% iron and combine our results with literature data for a range of ferropericlase compositions. Results from different studies show inconsistencies, caused by uncertainties inherent to experimental data. To overcome this, we use machine learning to infer the relationships between material properties, pressure and iron content. Our results show that the spin crossover would significantly alter properties of iron-rich ferropericlase in the deepest parts of the lower mantle. This may help to explain the anomalous behavior of seismic waves in regions near the core-mantle boundary.

Key Points:

- New time-resolved compression data on $(Mg_{0.60}Fe_{0.40})O$ and $(Mg_{0.41}Fe_{0.59})O$ across the spin crossover pressure range
- Effect of iron content on elastic properties of ferropericlase inferred from experimental data using machine learning techniques
- Spin crossover effects in iron-rich ferropericlase may contribute to seismic heterogeneities in the lowermost mantle

Supporting Information:

Supporting Information may be found in the online version of this article.

Correspondence to:

V. E. Trautner,
viktoria.trautner@earth.ox.ac.uk

Citation:

Trautner, V. E., Rijal, A., Plueckthun, C., Satta, N., Koemets, E., Buchen, J., et al. (2024). Iron content-dependence of ferropericlase elastic properties across the spin crossover from novel experiments and machine learning. *Geophysical Research Letters*, *51*, e2024GL111276. https://doi.org/10.1029/2024GL111276

Received 11 JUL 2024
Accepted 30 OCT 2024

Author Contributions:

Conceptualization: V. E. Trautner, A. Rijal, L. Cobden, H. Marquardt
Formal analysis: V. E. Trautner, A. Rijal
Funding acquisition: C. Plueckthun, L. Cobden, H. Marquardt
Investigation: V. E. Trautner, C. Plueckthun, N. Satta, E. Koemets, J. Buchen, B. Wang, H. Marquardt
Methodology: V. E. Trautner, A. Rijal
Project administration: V. E. Trautner, H. Marquardt
Resources: C. Plueckthun, K. Glazyrin, H. Marquardt
Software: V. E. Trautner, A. Rijal
Supervision: H. Marquardt
Visualization: V. E. Trautner

1. Introduction

Earth's lower mantle comprises over half of the planet's volume and is thought to predominantly consist of the two minerals bridgmanite and ferropericlase. For a pyrolitic bulk composition, $(Mg_{1-x}Fe_x)O$ ferropericlase constitutes approximately 18% by volume (Irifune et al., 2010) and is therefore expected to play a major role in the physical properties and geodynamic processes governing Earth's deep interior. Iron in ferropericlase undergoes a pressure-induced electronic spin transition from a high-spin (HS) to a low-spin (LS) state (Badro et al., 2003). The transition occurs gradually, with HS and LS iron atoms coexisting over a broad pressure/depth range that is referred to as the spin crossover region. Along a typical lower mantle geotherm, this region is expected to extend from approximately 1,500 km depth to the Core-Mantle Boundary (CMB) (Trautner et al., 2023). The spin crossover leads to a softening of the bulk modulus of ferropericlase (e.g., Marquardt et al., 2009; Méndez et al., 2022), with wide-ranging geophysical implications (e.g., Cammarano et al., 2010; Lin et al., 2013; Marquardt & Miyagi, 2015).

Writing – original draft: V. E. Trautner
Writing – review & editing:
V. E. Trautner, A. Rijal, N. Satta,
J. Buchen, K. Glazyrin, H. Marquardt

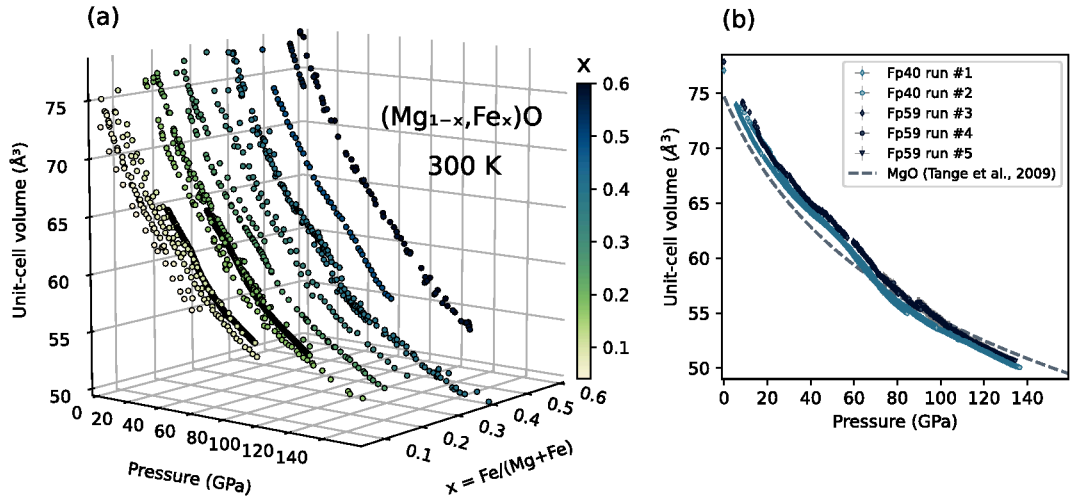

Figure 1. Experimental P-V-X_{Fe} data on $(Mg_{1-x}Fe_x)O$. (a) Overview of previously published P-V data from XRD measurements on ferropericlase with x_{Fe} = 0.04–0.6 (see Section 3.1 for references). Reported uncertainties are not shown for clarity. (b) Unit-cell volumes of $(Mg_{0.60}Fe_{0.40})O$ (Fp40, light symbols) and $(Mg_{0.41}Fe_{0.59})O$ (Fp59, dark symbols) as a function of pressure from our continuous compression experiments at room temperature. The effect of the spin crossover is clearly visible as an enhanced volume reduction. For reference, a third-order Birch-Murnaghan EOS for MgO from Tange et al. (2009) is included (dashed gray line).

Ferropericlase with approximately 20 at.% Fe (i.e., x_{Fe} = 0.2) is considered representative for most of the lower mantle (Irifune et al., 2010; Murakami et al., 2005; Sinmyo & Hirose, 2013) and has therefore been extensively studied (e.g., Lin et al., 2007; Mao et al., 2011; Méndez et al., 2022; Trautner et al., 2023; Wu et al., 2013). However, iron partitioning between ferropericlase and bridgmanite is expected to change with pressure, temperature and spin state, possibly increasing ferropericlase iron content up to 35 at.% at the base of the lower mantle (Muir & Brodholt, 2016). Evidence for a wide range of ferropericlase compositions has been found in super-deep diamond inclusions (Kiseeva et al., 2022) and the notion of a chemically heterogeneous lower mantle is becoming increasingly accepted. The anomalous seismic properties of Large Low Velocity Provinces (LLVPs) and Ultra Low Velocity Zones (ULVZs) are widely believed to have a thermo-chemical origin (Garnero et al., 2016). LLVPs are best explained by warm material enriched in iron and silicate (Deschamps et al., 2015), while ULVZs have been suggested to consist of chemically distinct, strongly iron-enriched material (e.g., Liu et al., 2016; Otsuka & Karato, 2012). Iron-enriched ferropericlase may play a major role in these observed heterogeneities, since iron partitions strongly into ferropericlase for high total iron contents (Muir & Brodholt, 2016) and the physical properties of iron-rich ferropericlase may account for the seismic characteristics of ULVZs (Finkelstein et al., 2018; Wicks et al., 2017; Yu & Garnero, 2018).

In light of the wide range of expected compositions of ferropericlase in Earth's lower mantle, a detailed understanding of the physical properties of ferropericlase as a function of iron content is essential. Changes as a result of the spin crossover are of particular interest. The spin crossover is known to shift to higher pressures with increasing iron content (e.g., Cheng et al., 2018; Glazyrin et al., 2017; Muir & Brodholt, 2015; Solomatova et al., 2016; Speziale et al., 2005), but the iron content-dependence of the elastic softening of ferropericlase is not well-constrained. While experimental high-pressure studies have been conducted for a range of ferropericlase compositions, data coverage is sparser for pressures relevant to the lowermost mantle (Figure 1a). Moreover, existing results are often inconsistent even at low pressures, likely due to inevitable experimental uncertainties and differences in experimental approaches and pressure scales used (Solomatova et al., 2016). In addition, the conventional approach to determine elastic properties of minerals by fitting data to an Equation of State (EOS) introduces potential biases in uncertainty quantification (Rijal et al., 2021) and is particularly problematic for ferropericlase due to its anomalous compression behavior across the spin crossover.

Here, we present new results on the compression behavior of $(Mg_{1-x}Fe_x)O$ with x_{Fe} = 0.40 and x_{Fe} = 0.59 across the spin crossover, employing time-resolved X-ray diffraction (XRD) in combination with continuous compression experiments in Diamond Anvil Cells (DACs). We combine our results with published pressure-

volume data on ferropericlase with $x_{Fe} = 0.04–0.6$ and use Mixture Density Networks (Rijal et al., 2021) to infer the relationship between pressure, unit-cell volume and iron content (P-V-X_{Fe}) of ferropericlase from the compiled data set. By applying machine learning techniques we can comprehensively integrate existing experimental data and quantify uncertainties. Furthermore, this approach allows us to derive the isothermal bulk modulus as a function of pressure and iron content, without imposing any a priori assumptions on the thermodynamic model or functional form of the EOS.

2. Materials and Methods

2.1. Experimental Details

Powdered samples of $(Mg_{0.604(4)}Fe_{0.396(4)})O$ and $(Mg_{0.409(4)}Fe_{0.591(4)})O$ (hereafter referred to as Fp40 and Fp59) were synthesized from stoichiometric mixtures of MgO and Fe_2O_3. The samples have a face-centered cubic structure at ambient conditions with zero-pressure volumes of 77.08 ± 0.03 $Å^3$ for Fp40 and 77.88 ± 0.06 $Å^3$ for Fp59 and $Fe^{3+}/\Sigma Fe$ of 0.071 ± 0.021 in Fp40 and 0.088 ± 0.015 in Fp40 (see Section S1 in Supporting Information S1 for details on sample synthesis and characterization). High-pressure experiments were conducted at room temperature in symmetric DACs prepared with rhenium gaskets. The cells were loaded with the sample powders, platinum foil as pressure marker and neon or helium gas as pressure-transmitting medium. Continuous compression experiments using a gas-membrane system were conducted at beamline P02.2 at PETRAIII, DESY, Germany in combination with time-resolved XRD measurements (Liermann et al., 2015). Details of all loadings and experiments are listed in Table S1 of Supporting Information S1 and described in Section S2 of Supporting Information S1. We collected quasi-continuous compression data on both sample compositions covering pressures from ~8 GPa to 135 GPa in five experimental runs with maximum compression rates of less than 0.15 GPa/s. The unit-cell volumes of ferropericlase and platinum were determined by fitting of diffraction peaks (Section S2 in Supporting Information S1) and experimental pressures were derived by employing a third-order Birch-Murnaghan EOS (Fei, Ricolleau, et al., 2007).

2.2. Mixture Density Networks

Since uncertainties are inherent to experimental measurements, inferring the P-V-X_{Fe} relationship from experimental data is a probabilistic inverse problem and the solution is the posterior probability density function (pdf) for volume. We seek to solve this inverse problem using a neural network-based approach called Mixture Density Network (MDN) (Bishop, 1995), where a conventional feed-forward neural network is combined with a Gaussian mixture model to find the posterior pdf at a given pressure and iron content (Rijal et al., 2021). MDNs are flexible and can approximate arbitrary pdfs, making them well-suited to investigate the compression behavior of ferropericlase across the spin crossover.

Collated experimental P-V-X_{Fe} data for ferropericlase (Figure S4, Table S2, and Section S5 in Supporting Information S1) is used to train the MDNs. Training (≈70%), monitoring (≈20%) and test (≈10%) sets are randomly generated from the total data set. The loss function used to compute the difference between output and target is described in detail in Rijal et al. (2021). Once training of an MDN begins, this function is summed over all data in the training set to provide the average training error and minimized iteratively. The same error function is used to calculate monitoring and test set errors. The monitoring set is used to monitor overfitting of the training data by the MDN. The test set is not seen by the network during training and is used to evaluate the prediction performance of the trained MDN and assign a weight to it. We train a large number of MDNs (10^3) and combine their predicted pdfs by a weighted sum (Rijal et al., 2021). See Section S5 in Supporting Information S1 for details on the setup and training of the MDNs.

The isothermal bulk modulus K_T can be directly derived from the pressure-volume curve using the identity: $K_T = -V \cdot \left(\frac{\partial P}{\partial V}\right)_T$. To constrain K_T of ferropericlase from the P-V-X_{Fe} relationships predicted by the MDNs, we calculate the conditional mean volume for any given pressure and iron content from each trained MDN, which corresponds to the standard output of a feed-forward neural network. Then we obtain the derivative of the *V(P)* curve by perturbing pressure, allowing us to compute K_T (Rijal et al., 2021). Since we have trained 10^3 networks, we can estimate uncertainty from the spread in the derived K_T values and calculate the weighted average using the weights obtained from the test set error.

3. Results and Discussion

3.1. P-V-X_{Fe} Relationship of $(Mg_{1-x}Fe_x)O$

The collected quasi-continuous compression curves of $(Mg_{0.60}Fe_{0.40})O$ and $(Mg_{0.41}Fe_{0.59})O$ are shown in Figure 1b. Peak-broadening indicates the onset of a cubic-rhombohedral transition for both Fp40 and Fp59 at about 30 GPa (Figures S1e and S1f in Supporting Information S1), but no peak-splitting was observed in the XRD images. We did not find significant effects of the rhombohedral distortion on the unit-cell volumes (Figure S2, and Section S4 in Supporting Information S1), although it appears to reduce deviatoric stresses (Figure S1, and Section S3 in Supporting Information S1). The presence of ~8% Fe^{3+} in both Fp40 and Fp59 is expected to reduce the measured volumes slightly with respect to stoichiometric $(Mg_{1-x}Fe_x)O$ (Jacobsen et al., 2002). Such Fe^{3+}-contents are common for Fe-rich ferropericlase samples and may well exist at lower mantle conditions (Sinmyo et al., 2008). We observe an enhanced volume contraction during the compression of both Fp40 and Fp59 (Figure 1b), which is attributed to the spin crossover of Fe^{2+}. For Fp40 the spin crossover occurs over a pressure range of about 50–85 GPa, whereas for Fp59 it shifts to higher pressure and broadens to about 60–110 GPa (Figures S1c and S1d, Section S3 in Supporting Information S1). We note that the two compression runs on Fp40 are in excellent agreement above approximately 30 GPa, but they deviate at lower pressures, which is highlighted by the high data density obtained in our time-resolved XRD measurements. Given that experimental conditions were the same for both runs, the observed differences are likely the result of deviatoric stresses (see Section S3, Figure S1a and S1b in Supporting Information S1).

To investigate P-V-X_{Fe} relationships of ferropericlase we combine our experimental results with previously published high-pressure XRD data on $(Mg_{1-x}Fe_x)O$ with x_{Fe} = 0.04–0.60 (Chen et al., 2012;; Fei et al., 1992; Fei & Zhang et al., 2007; Glazyrin et al., 2017; Hamada et al., 2021; Jacobsen et al., 2002, 2005; Kantor et al., 2006; Komabayashi et al., 2010; Lin et al., 2005; Mao et al., 2011; Marquardt et al., 2009; Matsui et al., 2012; Méndez et al., 2022; Richet et al., 1989; Rosenhauer et al., 1976; Solomatova et al., 2016; Speziale et al., 2007; Westrenen et al., 2005; Yang et al., 2015, 2016; Zhang & Kostak, 2002; Zhuravlev et al., 2010) (Figure 1). Experimental approaches vary widely between studies (Table S2 in Supporting Information S1) and although the compiled data show a clear trend overall, quantitative differences and inconsistencies are apparent, limiting the robustness in obtained P-V-X_{Fe} relationships.

To map out how iron content affects the elastic behavior of ferropericlase across the spin crossover we have employed machine learning techniques, that allow comprehensive integration of all existing experimental results and unbiased uncertainty quantification of the inferred relationship. The MDN-predicted unit-cell volume pdfs for different iron contents are presented in Figure 2. The effect of the spin crossover is clearly visible for all compositions as an enhanced volume contraction, with the onset shifting to higher pressures with iron content. The width of the posterior volume pdfs predicted by the MDNs is an indication for uncertainty and is expected to be greater in regions where experimental data coverage is sparse, measurement errors are high or where discrepancies between published data are large. For all compositions, the pdfs are wider in the spin crossover pressure range (Figure 2). Glazyrin et al. (2016) suggested that the spin crossover is sensitive to nonhydrostatic stresses, which may lead to a larger data spread in this region and explain the greater uncertainties. The pdfs for x_{Fe} = 0.4 and x_{Fe} = 0.6 are comparatively wide and bimodal between approximately 5–35 GPa, which is caused by large discrepancies between data sets from different studies (Figure S4 in Supporting Information S1). The larger ionic radius of HS Fe^{2+} compared to Mg^{2+} (Shannon, 1976) may make the volume of iron-rich ferropericlase more sensitive to non-hydrostatic stresses at pressures below the spin crossover, with the rhombohedral distortion helping to accommodate these stresses.

3.2. Spin Crossover-Induced Bulk Modulus Softening

Most previous attempts to constrain the bulk modulus across the spin crossover from experimental *V(P)* data are based on fitting the data to fixed functional forms for HS and LS ferropericlase, with inherent biases resulting from the choice of functional, use of priors or prior windows and/or specifying the spin crossover pressure range (e.g., Chen et al., 2012; Lin et al., 2005; Mao et al., 2011; Marquardt et al., 2009; Solomatova et al., 2016). With our approach, P-V-X_{Fe} relationships are implicitly learned from data during the training of the MDNs and bulk moduli are computed directly from the *P(V)* derivative of the mapping without any a priori constraints.

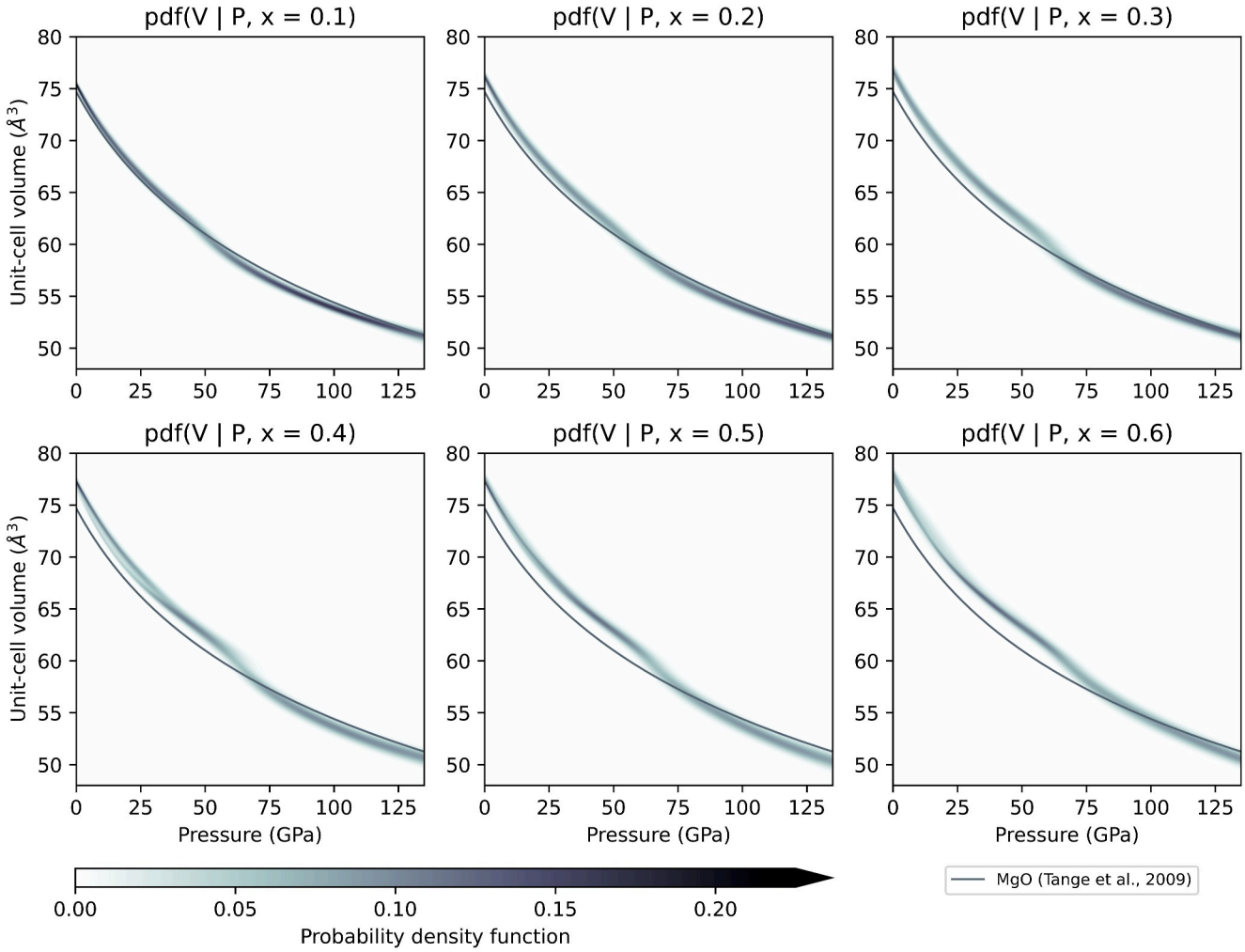

Figure 2. Pdfs for the unit-cell volume of $(Mg_{1-x}Fe_x)O$ as a function of pressure predicted by MDNs for different iron contents. The MDNs were trained using experimental high-pressure data with x_{Fe} = 0.04–0.6. The color scale corresponds to the value of the pdfs and the compression curve of MgO (Tange et al., 2009) is shown as a gray line for reference.

The bulk modulus values obtained from all 10^3 MDNs are plotted as a function of pressure in Figure 3 as 2D histograms for different iron contents. We find that the values predicted by the networks are largely consistent, producing well-defined $K_T(P)$ curves. However, the spread in values, and thus uncertainty, dramatically increases at high pressures, particularly for compositions where experimental data coverage is sparse. The means and standard deviations of the bulk modulus distributions are shown in Figure 4b. The deviations between data sets from different studies on $x_{Fe} \approx 0.6$ at pressures <30 GPa (Figure S4 in Supporting Information S1) are captured by the larger uncertainties. While the bulk moduli inferred by the MDNs are very close to those predicted for MgO (Tange et al., 2009) at low pressures, a spin crossover-induced softening of the bulk modulus is clearly visible with increasing pressure for all compositions. The only experimental constraints on the bulk modulus of ferropericlase not derived from XRD measurements are obtained through spectroscopic methods. With the exception of data from Antonangeli et al. (2011), spectroscopic measurements also show a softening of the bulk modulus across the spin crossover for x_{Fe} = 0.06 (Crowhurst et al., 2008) and x_{Fe} = 0.08 (Yang et al., 2015). These results are in reasonable agreement with our MDN results for a similar composition (x_{Fe} = 0.1, Figures 3 and 4b).

The onset of the spin crossover shifts to higher pressures with increasing iron content by about 15 GPa between x_{Fe} = 0.05 and x_{Fe} = 0.6. We also observe a broadening of the bulk modulus softening with iron content, indicating an increase in the spin crossover pressure range, qualitatively consistent with previous studies (Solomatova et al., 2016 and references therein). The pressure where the bulk modulus shows the largest softening

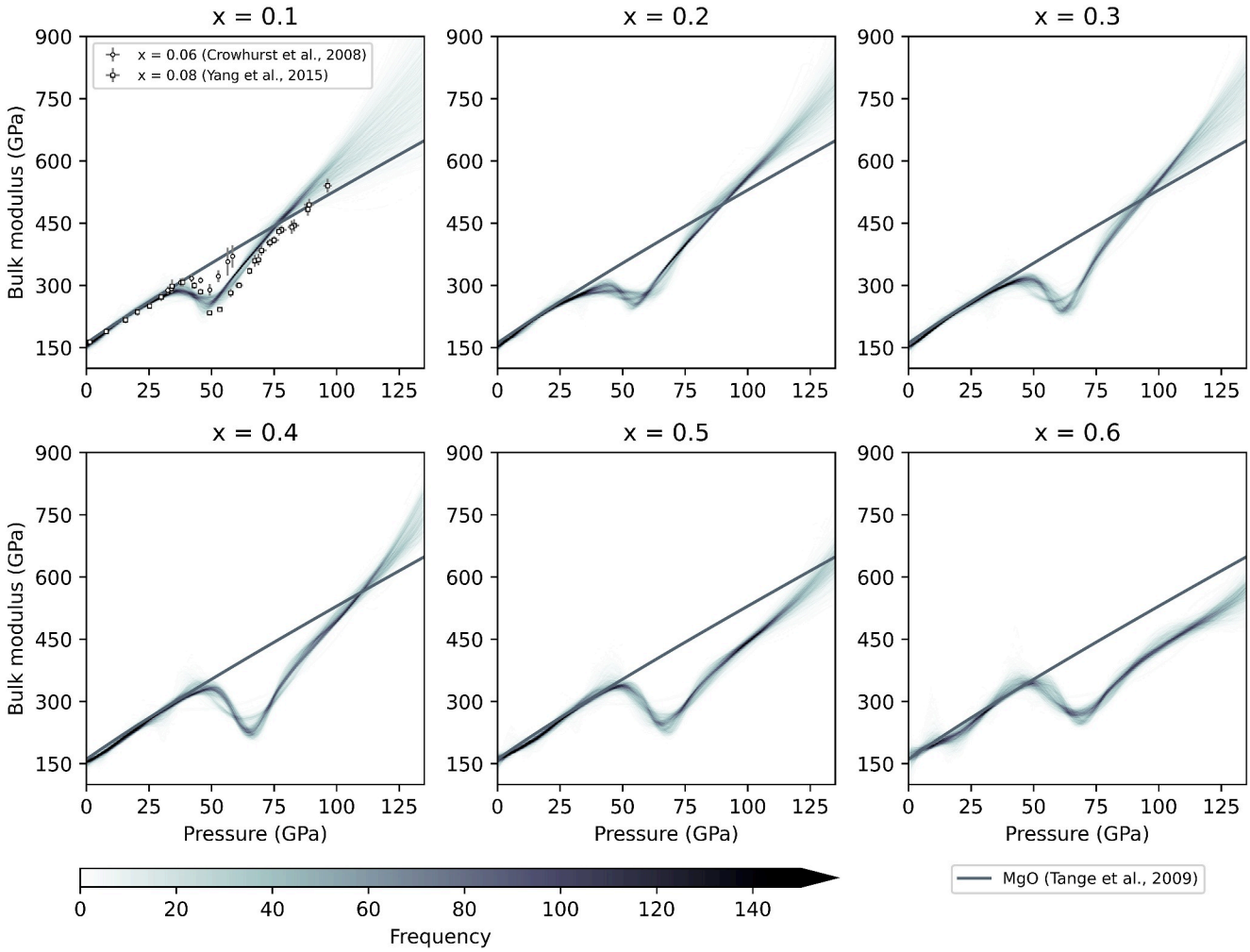

Figure 3. Frequency distribution of the isothermal bulk modulus values for $(Mg_{1-x}Fe_x)O$ as a function of pressure predicted by 10^3 trained MDNs for different iron contents. The frequency counts for the predicted values are at intervals of 0.1 GPa for pressure and 2 GPa for bulk modulus and the color scale corresponds to the number of MDNs predicting that value. The bulk modulus of MgO (Tange et al., 2009) is shown for reference (gray line). Adiabatic bulk modulus values obtained from optical spectroscopy measurements (Crowhurst et al., 2008; Yang et al., 2015) are compared to the MDN-predicted values for $x_{Fe} = 0.1$.

increases with iron content from 46.0 GPa for $x_{Fe} = 0.05$ to 68.3 GPa for $x_{Fe} = 0.6$. While the correlation between iron content and magnitude of maximal softening is positive for low iron contents, it becomes negative at high iron contents (inset Figure 4b). The shape and magnitude of the bulk modulus softening is directly related to the magnitude of the volume reduction between HS and LS states and the pressure range over which it occurs. We find that the degree of maximal softening is largest for $x_{Fe} = 0.4$, which may be the result of a trade-off between an increase in volume reduction for higher iron contents due to the larger number of iron atoms undergoing a spin transition and a broadening of the spin crossover region, leading to a more gradual decrease in volume with pressure. The broadness of the spin crossover at room temperature is attributed to a favorable enthalpy of mixing ΔH_{mix} of HS and LS iron (Holmström & Stixrude, 2015). The arrangement of iron atoms affects the magnitude of ΔH_{mix}, with LS atoms stabilizing neighboring on-axis HS atoms to higher pressures (see Méndez et al., 2022). For higher iron contents, the number of neighboring on-axis iron atoms should increase, which may be the cause of the broadening of the spin crossover region with iron content.

4. Geophysical Implications

The P-K_T-X_{Fe} relationship of ferropericlase inferred by the MDNs indicates that the effect of the spin crossover on the bulk modulus is largest for $x_{Fe} \approx 0.4$ (inset Figure 4b). To assess potential implications for the interpretation of seismological observations of the lower mantle, it must be taken into account that the spin crossover

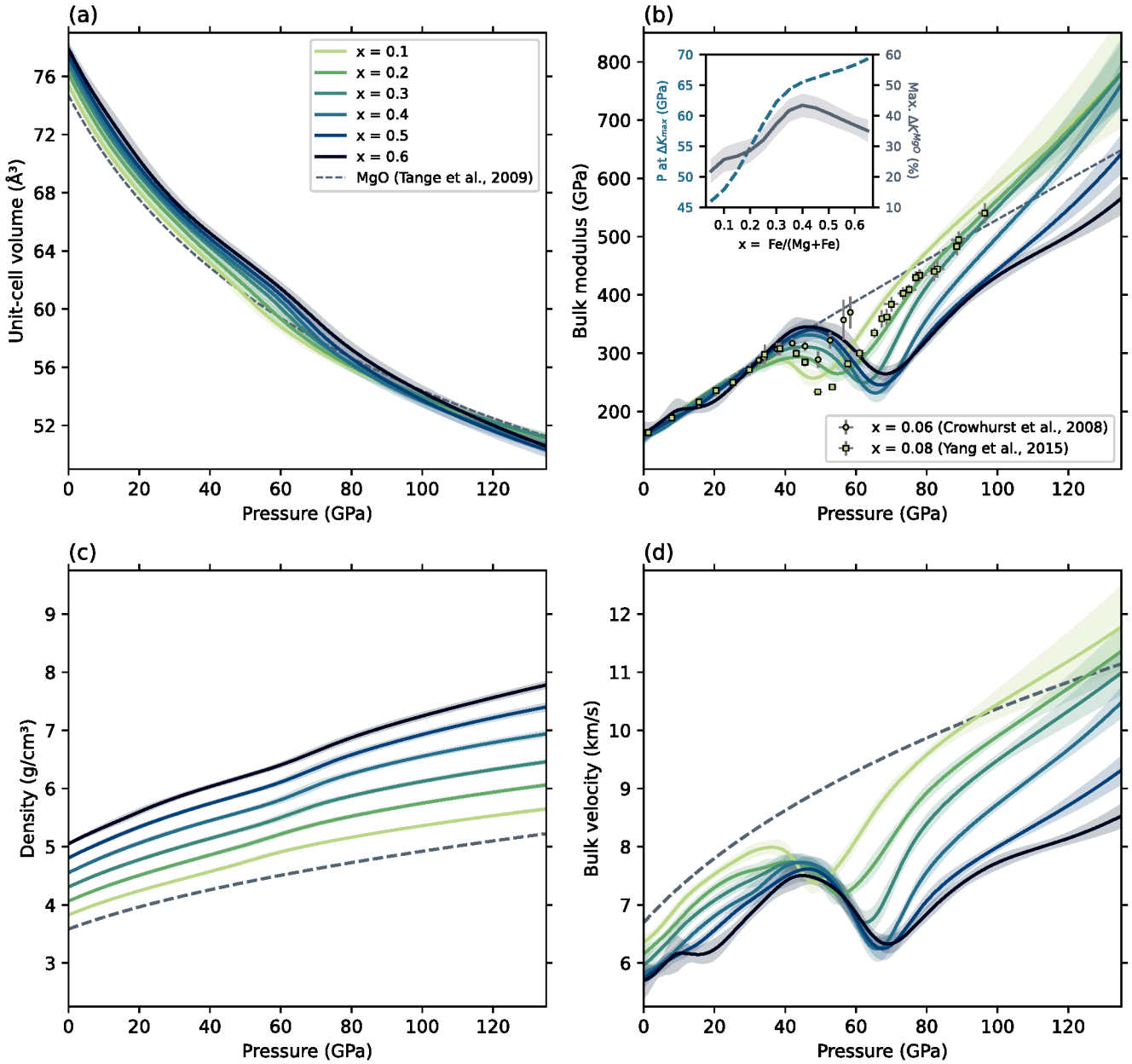

Figure 4. MDN predictions of mean (a) unit-cell volume, (b) isothermal bulk modulus, (c) density and (d) bulk sound velocity of $(Mg_{1-x}Fe_x)O$ as a function of pressure. Colors indicate iron contents and shaded areas correspond to one standard deviation from the mean. Properties for MgO derived from a third-order Birch-Murnaghan EOS (Tange et al., 2009) are shown for reference as dashed gray lines. In (b), adiabatic bulk modulus values obtained from optical spectroscopy measurements (Crowhurst et al., 2008; Yang et al., 2015) are shown for comparison. Inset: percentage of maximal bulk modulus softening with respect to MgO and the corresponding pressure as a function of iron content.

broadens and shifts to higher pressures with temperature (e.g., Trautner et al., 2023; Wu et al., 2013; Yang et al., 2021). Assuming the effects of temperature are comparable for $x_{Fe} = 0.2$ and $x_{Fe} = 0.4$ and using the temperature dependency predicted by Méndez et al. (2022) and Trautner et al. (2023), the maximum bulk modulus softening in $x_{Fe} = 0.4$ would occur at approximately 130 GPa for a mantle temperature of 2900 K, corresponding to a depth of about 2,750 km. These conditions are similar to those near the CMB along a typical geotherm (Davies et al., 2012), suggesting that the physical properties of a phase assemblage containing moderately iron-enriched ferropericlase at the base of the lower mantle would be markedly affected by the spin crossover. This is an important finding since iron is expected to partition strongly into ferropericlase for iron-rich bulk compositions near the CMB (Muir & Brodholt, 2016) and the presence of iron-enriched ferropericlase in the lowermost mantle

has been hypothesized to explain the seismic anomalies observed in ULVZs (e.g., Liu et al., 2016; Otsuka & Karato, 2012; Wicks et al., 2017; Yu & Garnero, 2018).

The compressional (V_P) and bulk (V_C) seismic wave velocities of ferropericlase are strongly affected by the spin crossover (e.g., Crowhurst et al., 2008; Marquardt et al., 2009; Wu et al., 2013; Yang et al., 2015), since they directly depend on the bulk modulus: $V_P^2 = \frac{K+\frac{4}{3}G}{\rho}$ and $V_C^2 = \frac{K}{\rho}$, where G is the shear modulus and ρ is density. Calculating compressional wave velocities requires constraints on the shear modulus, but density and bulk velocities can be directly computed from the MDN-predicted mean unit-cell volumes and bulk moduli (Figure 4). Uncertainties are propagated from the standard deviations of the volume pdfs (Figure 2) and distributions of K_T values (Figure 3). We find that density increases with iron content and that the density contrast between iron-poor and iron-rich ferropericlase is larger at high pressures, that is, in LS state (Figure 4c). Bulk velocities decrease with iron content in HS and LS state and show a similar softening as the bulk modulus in the spin crossover pressure range (Figure 4d).

Shear wave velocities (V_S) depend only on shear modulus and density $\left(V_S^2 = \frac{G}{\rho}\right)$. Previous investigations have shown that the shear modulus of ferropericlase is not sensitive to the spin crossover, systematically increasing with pressure and decreasing with temperature and iron content (Marquardt et al., 2009; Muir & Brodholt, 2015; Wicks et al., 2017; Yang et al., 2015, 2016). The contrasting effects of the spin crossover on shear velocities versus compressional and bulk velocities result in a characteristically high ratio of V_S over V_P and a strong negative correlation between V_S and V_C (Marquardt et al., 2009; Trautner et al., 2023). These are features commonly observed in seismic tomography models of the lowermost mantle for which the post-perovskite phase has been suggested as an explanation (Koelemeijer et al., 2018). Our findings of the spin crossover shifting to higher pressures with iron content and amplification of the softening for moderately iron-enriched compositions indicate that the spin crossover may contribute significantly to anomalous seismic features observed at the base of the lower mantle and should be considered in seismic inversions.

5. Conclusions

By using machine learning techniques to infer the P-V-X_{Fe} relationship of ferropericlase from a combination of new experimental results and literature data, we show how the effects of the spin crossover on bulk modulus, density and bulk velocity change with iron content. This approach avoids prescribing an explicit functional form and provides us with uncertainties that reflect the consistency between data from different sources, without any potential biases introduced by subjective selection of data or the choice of a particular EOS (Rijal et al., 2021). Our results can improve uncertainty quantification in the interpretation of seismic observations and provide constraints for thermodynamic databases and geodynamic models. The shift of the spin crossover to higher pressures with iron content and the amplified bulk modulus softening for moderate iron contents around $x_{Fe} = 0.4$ suggest that seismic properties of the lowermost mantle may be strongly affected by the spin crossover. Once sufficient data is available, the MDN-based approach applied here can be extended to temperature (T) and used to predict the properties of ferropericlase in P-T-X_{Fe} space. Integrating MDNs with theoretical calculations (e.g., Muir & Brodholt, 2015) and/or physical laws as regularization agents, for example, by combining them with Physics-Informed Neural Networks (Raissi et al., 2019) may provide additional constraints.

Data Availability Statement

Separate tables with the experimental pressure-volume data, MDN-predicted volume pdfs and mean volumes and bulk moduli are available at the Figshare repository via https://doi.org/10.6084/m9.figshare.27194055.v1 (Trautner, 2024).

Acknowledgments
This research received funding through the European Union's Horizon 2020 research and innovation programme (ERC Grant 864877), as well as UKRI STFC Grant ST/V000527/1. CP acknowledges support from the DFG Core Facilities Programme (project KO-5262/1) for sample synthesis and characterization. AR and LC received funding through the Dutch Research Council (NWO, Grant 016.Vidi.171.022). The authors acknowledge beamline P02.2, PETRA III, DESY (Hamburg, Germany), a member of the Helmholtz Association HGF, for the provision of experimental facilities and thank Nico Giordano and Timofey Fedotenko for help with gas-loading. We acknowledge the use of the University of Oxford Advanced Research Computing (ARC) facility in carrying out this work. http://dx.doi.org/10.5281/zenodo.22558. VT is grateful to Andrew Matzen for assistance with microprobe analyses and Andrew Walker for help with using ARC. We thank Jie Deng and an anonymous reviewer for their constructive comments.

References

Antonangeli, D., Siebert, J., Aracne, C. M., Farber, D. L., Bosak, A., Hoesch, M., et al. (2011). Spin crossover in ferropericlase at high pressure: A seismologically transparent transition? *Science*, *331*(6013), 64–67. https://doi.org/10.1126/science.1198429

Badro, J., Fiquet, G., Guyot, F., Rueff, J.-P., Struzhkin, V. V., Vankó, G., & Monaco, G. (2003). Iron partitioning in earth's mantle: Toward a deep lower mantle discontinuity. *Science*, *300*(5620), 789–791. https://doi.org/10.1126/science.1081311

Bishop, C. M. (1995). *Neural networks for pattern recognition*. Oxford University Press.

Cammarano, F., Marquardt, H., Speziale, S., & Tackley, P. J. (2010). Role of iron-spin transition in ferropericlase on seismic interpretation: A broad thermochemical transition in the mid mantle? *Geophysical Research Letters*, *37*(3), L03308. https://doi.org/10.1029/2009gl041583

Chen, B., Jackson, J. M., Sturhahn, W., Zhang, D., Zhao, J., Wicks, J. K., & Murphy, C. A. (2012). Spin crossover equation of state and sound velocities of ($Mg_{0.65}Fe_{0.35}$)O ferropericlase to 140 GPa. *Journal of Geophysical Research*, *117*(B8), B08208. https://doi.org/10.1029/2012jb009162

Cheng, Y., Wang, X., Zhang, J., Yang, K., Zhang, C., Zeng, Z., & Lin, H. (2018). Investigation of iron spin crossover pressure in Fe-bearing MgO using hybrid functional. *Journal of Physics: Condensed Matter*, *30*(15), 155403. https://doi.org/10.1088/1361-648x/aab4b5

Crowhurst, J. C., Brown, J. M., Goncharov, A. F., & Jacobsen, S. D. (2008). Elasticity of (Mg,Fe)O through the spin transition of iron in the lower mantle. *Science*, *319*(5862), 451–453. https://doi.org/10.1126/science.1149606

Davies, D. R., Goes, S., Davies, J. H., Schuberth, B. S. A., Bunge, H. P., & Ritsema, J. (2012). Reconciling dynamic and seismic models of Earth's lower mantle: The dominant role of thermal heterogeneity. *Earth and Planetary Science Letters*, *353–354*, 253–269. https://doi.org/10.1016/j.epsl.2012.08.016

Deschamps, F., Li, Y., & Tackley, P. J. (2015). Large-scale thermo-chemical structure of the deep mantle: Observations and models. In (Ed), *The Earth's Heterogeneous Mantle* (pp. 479–515). Springer International Publishing.

Fei, Y., Mao, H.-K., Shu, J., & Hu, J. (1992). P-V-T equation of state of magnesiowüstite ($Mg_{0.6}Fe_{0.4}$)O. *Physics and Chemistry of Minerals*, *18*(7), 416–422. https://doi.org/10.1007/BF00200964

Fei, Y., Ricolleau, A., Frank, M., Mibe, K., Shen, G., & Prakapenka, V. (2007). Toward an internally consistent pressure scale. *Proceedings of the National Academy of Sciences of the U S A*, *104*(22), 9182–9186. https://doi.org/10.1073/pnas.0609013104

Fei, Y., Zhang, L., Corgne, A., Watson, H., Ricolleau, A., Meng, Y., & Prakapenka, V. (2007). Spin transition and equations of state of (Mg, Fe)O solid solutions. *Geophysical Research Letters*, *34*(17), L17307. https://doi.org/10.1029/2007gl030712

Finkelstein, G. J., Jackson, J. M., Said, A., Alatas, A., Leu, B. M., Sturhahn, W., & Toellner, T. S. (2018). Strongly anisotropic magnesiowüstite in Earth's lower mantle. *Journal of Geophysical Research: Solid Earth*, *123*(6), 4740–4750. https://doi.org/10.1029/2017jb015349

Garnero, E. J., Mcnamara, A. K., & Shim, S.-H. (2016). Continent-sized anomalous zones with low seismic velocity at the base of Earth's mantle. *Nature Geoscience*, *9*(7), 481–489. https://doi.org/10.1038/ngeo2733

Glazyrin, K., Miyajima, N., Smith, J. S., & Lee, K. K. M. (2016). Compression of a multiphase mantle assemblage: Effects of undesirable stress and stress annealing on the iron spin state crossover in ferropericlase. *Journal of Geophysical Research: Solid Earth*, *121*(5), 3377–3392. https://doi.org/10.1002/2015JB012321

Glazyrin, K., Sinmyo, R., Bykova, E., Bykov, M., Cerantola, V., Longo, M., et al. (2017). Critical behavior of $Mg_{1-x}Fe_xO$ at the pressure-induced iron spin-state crossover. *Physical Review B*, *95*(21), 214412. https://doi.org/10.1103/physrevb.95.214412

Hamada, M., Kamada, S., Ohtani, E., Sakamaki, T., Mitsui, T., Masuda, R., et al. (2021). Synchrotron Mössbauer spectroscopic and X-ray diffraction study of ferropericlase in the high-pressure range of the lower mantle region. *Physical Review B*, *103*(17), 174108. https://doi.org/10.1103/PhysRevB.103.174108

Holmström, E., & Stixrude, L. (2015). Spin crossover in ferropericlase from first-principles molecular dynamics. *Physical Review Letters*, *114*(11), 117202. https://doi.org/10.1103/PhysRevLett.114.117202

Irifune, T., Shinmei, T., McCammon, C. A., Miyajima, N., Rubie, D. C., & Frost, D. J. (2010). Iron partitioning and density changes of pyrolite in Earth's lower mantle. *Science*, *327*(5962), 193–195. https://doi.org/10.1126/science.1181443

Jacobsen, S. D., Lin, J.-F., Angel, R. J., Shen, G., Prakapenka, V. B., Dera, P., et al. (2005). Single-crystal synchrotron X-ray diffraction study of wüstite and magnesiowüstite at lower-mantle pressures. *Journal of Synchrotron Radiation*, *12*(5), 577–583. https://doi.org/10.1107/s0909049505022326

Jacobsen, S. D., Reichmann, H.-J., Spetzler, H. A., Mackwell, S. J., Smyth, J. R., Angel, R. J., & McCammon, C. A. (2002). Structure and elasticity of single-crystal (Mg,Fe)O and a new method of generating shear waves for gigahertz ultrasonic interferometry. *Journal of Geophysical Research*, *107*(B2), ECV4-1–ECV4-14. https://doi.org/10.1029/2001jb000490

Kantor, I., Dubrovinsky, L., McCammon, C. A., Kantor, A., Pascarelli, S., Aquilanti, G., et al. (2006). Pressure-induced phase transition in $Mg_{0.8}Fe_{0.2}O$ ferropericlase. *Physics and Chemistry of Minerals*, *33*(1), 35–44. https://doi.org/10.1007/s00269-005-0052-z

Kiseeva, E. S., Korolev, N., Koemets, I., Zedgenizov, D. A., Unitt, R., McCammon, C., et al. (2022). Subduction-related oxidation of the sub-lithospheric mantle evidenced by ferropericlase and magnesiowüstite diamond inclusions. *Nature Communications*, *13*(1), 7517. https://doi.org/10.1038/s41467-022-35110-x

Koelemeijer, P., Schuberth, B. S. A., Davies, D. R., Deuss, A., & Ritsema, J. (2018). Constraints on the presence of post-perovskite in Earth's lowermost mantle from tomographic-geodynamic model comparisons. *Earth and Planetary Science Letters*, *494*, 226–238. https://doi.org/10.1016/j.epsl.2018.04.056

Komabayashi, T., Hirose, K., Nagaya, Y., Sugimura, E., & Ohishi, Y. (2010). High-temperature compression of ferropericlase and the effect of temperature on iron spin transition. *Earth and Planetary Science Letters*, *297*(3–4), 691–699. https://doi.org/10.1016/j.epsl.2010.07.025

Liermann, H.-P., Konôpková, Z., Morgenroth, W., Glazyrin, K., Bednarčik, J., Mcbride, E. E., et al. (2015). The extreme conditions beamline P02.2 and the extreme conditions science infrastructure at PETRA III. *Journal of Synchrotron Radiation*, *22*(4), 908–924. https://doi.org/10.1107/s1600577515005937

Lin, J.-F., Speziale, S., Mao, Z., & Marquardt, H. (2013). Effects of the electronic spin transitions of iron in lower mantle minerals: Implications for deep mantle geophysics and geochemistry. *Reviews of Geophysics*, *51*(2), 244–275. https://doi.org/10.1002/rog.20010

Lin, J.-F., Struzhkin, V. V., Jacobsen, S. D., Hu, M. Y., Chow, P., Kung, J., et al. (2005). Spin transition of iron in magnesiowüstite in the Earth's lower mantle. *Nature*, *436*(7049), 377–380. https://doi.org/10.1038/nature03825

Lin, J.-F., Vankó, G., Jacobsen, S. D., Iota, V., Struzhkin, V. V., Prakapenka, V. B., et al. (2007). Spin transition zone in Earth's lower mantle. *Science*, *317*(5845), 1740–1743. https://doi.org/10.1126/science.1144997

Liu, J., Li, J., Hrubiak, R., & Smith, J. S. (2016). Origins of ultralow velocity zones through slab-derived metallic melt. *Proceedings of the National Academy of Sciences*, *113*(20), 5547–5551. https://doi.org/10.1073/pnas.1519540113

Mao, Z., Lin, J.-F., Liu, J., & Prakapenka, V. B. (2011). Thermal equation of state of lower-mantle ferropericlase across the spin crossover. *Geophysical Research Letters*, *38*(23), L23308. https://doi.org/10.1029/2011gl049915

Marquardt, H., & Miyagi, L. (2015). Slab stagnation in the shallow lower mantle linked to an increase in mantle viscosity. *Nature Geoscience*, *8*(4), 311–314. https://doi.org/10.1038/ngeo2393

Marquardt, H., Speziale, S., Reichmann, H. J., Frost, D. J., & Schilling, F. R. (2009). Single-crystal elasticity of ($Mg_{0.9}Fe_{0.1}$)O to 81 GPa. *Earth and Planetary Science Letters*, *287*(3–4), 345–352. https://doi.org/10.1016/j.epsl.2009.08.017

Matsui, M., Ito, E., Yamazaki, D., Yoshino, T., Guo, X., Shan, S., et al. (2012). Static compression of ($Mg_{0.83}$,$Fe_{0.17}$)O and ($Mg_{0.75}$,$Fe_{0.25}$)O ferropericlase up to 58 GPa at 300, 700, and 1100 K. *American Mineralogist*, *97*(1), 176–183. https://doi.org/10.2138/am.2012.3937

Méndez, A. S. J., Stackhouse, S., Trautner, V., Wang, B., Satta, N., Kurnosov, A., et al. (2022). Broad elastic softening of (Mg,Fe)O ferropericlase across the iron spin crossover and a mixed-spin lower mantle. *Journal of Geophysical Research: Solid Earth*, *127*(8), e2021JB023832. https://doi.org/10.1029/2021jb023832

Muir, J. M. R., & Brodholt, J. P. (2015). Elastic properties of ferropericlase at lower mantle conditions and its relevance to ULVZs. *Earth and Planetary Science Letters*, *417*, 40–48. https://doi.org/10.1016/j.epsl.2015.02.023

Muir, J. M. R., & Brodholt, J. P. (2016). Ferrous iron partitioning in the lower mantle. *Physics of the Earth and Planetary Interiors*, *257*, 12–17. https://doi.org/10.1016/j.pepi.2016.05.008

Murakami, M., Hirose, K., Sata, N., & Ohishi, Y. (2005). Post-perovskite phase transition and mineral chemistry in the pyrolitic lowermost mantle. *Geophysical Research Letters*, *32*(3). https://doi.org/10.1029/2004gl021956

Otsuka, K., & Karato, S.-I. (2012). Deep penetration of molten iron into the mantle caused by a morphological instability. *Nature*, *492*(7428), 243–246. https://doi.org/10.1038/nature11663

Raissi, M., Perdikaris, P., & Karniadakis, G. E. (2019). Physics-informed neural networks: A deep learning framework for solving forward and inverse problems involving nonlinear partial differential equations. *Journal of Computational Physics*, *378*, 686–707. https://doi.org/10.1016/j.jcp.2018.10.045

Richet, P., Mao, H. K., & Bell, P. M. (1989). Bulk moduli of magnesiowüstites from static compression measurements. *Journal of Geophysical Research*, *94*(B3), 3037–3045. https://doi.org/10.1029/jb094ib03p03037

Rijal, A., Cobden, L., Trampert, J., Jackson, J. M., & Valentine, A. (2021). Inferring material properties of the lower mantle minerals using Mixture Density Networks. *Physics of the Earth and Planetary Interiors*, *319*, 106784. https://doi.org/10.1016/j.pepi.2021.106784

Rosenhauer, M., Mao, H. K., & Woermann, E. (1976). *Compressibility of magnesiowüstite ($Mg_{0.6}Fe_{0.4}$)O to 264 kbar* (Vol. 75, pp. 513–515). Year book/Carnegie Institution of Washington: v.75 1975/1976.

Shannon, R. D. (1976). Revised effective ionic radii and systematic studies of interatomic distances in halides and chalcogenides. *Acta Crystallographica Section A*, *32*(5), 751–767. https://doi.org/10.1107/S0567739476001551

Sinmyo, R., & Hirose, K. (2013). Iron partitioning in pyrolitic lower mantle. *Physics and Chemistry of Minerals*, *40*(2), 107–113. https://doi.org/10.1007/s00269-012-0551-7

Sinmyo, R., Ozawa, H., Hirose, K., Yasuhara, A., Endo, N., Sata, N., & Ohishi, Y. (2008). Ferric iron content in (Mg,Fe)SiO_3 perovskite and post-perovskite at deep lower mantle conditions. *American Mineralogist*, *93*(11–12), 1899–1902. https://doi.org/10.2138/am.2008.2806

Solomatova, N. V., Jackson, J. M., Sturhahn, W., Wicks, J. K., Zhao, J., Toellner, T. S., et al. (2016). Equation of state and spin crossover of (Mg, Fe)O at high pressure, with implications for explaining topographic relief at the core-mantle boundary. *American Mineralogist*, *101*(5), 1084–1093. https://doi.org/10.2138/am-2016-5510

Speziale, S., Lee, V. E., Clark, S. M., Lin, J. F., Pasternak, M. P., & Jeanloz, R. (2007). Effects of Fe spin transition on the elasticity of (Mg, Fe)O magnesiowüstites and implications for the seismological properties of the Earth's lower mantle. *Journal of Geophysical Research*, *112*(B10), B10212. https://doi.org/10.1029/2006jb004730

Speziale, S., Milner, A., Lee, V. E., Clark, S. M., Pasternak, M. P., & Jeanloz, R. (2005). Iron spin transition in Earth's mantle. *Proceedings of the National Academy of Sciences*, *102*(50), 17918–17922. https://doi.org/10.1073/pnas.0508919102

Tange, Y., Nishihara, Y., & Tsuchiya, T. (2009). Unified analyses for P-V-T equation of state of MgO: A solution for pressure-scale problems in high P-T experiments. *Journal of Geophysical Research*, *114*(B3). https://doi.org/10.1029/2008jb005813

Trautner, V. E. (2024). Data from Trautner et al. (2024) [Dataset]. *Figshare*. https://doi.org/10.6084/m9.figshare.27194055.v1

Trautner, V. E., Stackhouse, S., Turner, A. R., Koelemeijer, P., Davies, D. R., Méndez, A. S. J., et al. (2023). Compressibility of ferropericlase at high-temperature: Evidence for the iron spin crossover in seismic tomography. *Earth and Planetary Science Letters*, *618*, 118296. https://doi.org/10.1016/j.epsl.2023.118296

Westrenen, W. V., Li, J., Fei, Y., Frank, M. R., Hellwig, H., Komabayashi, T., et al. (2005). Thermoelastic properties of ($Mg_{0.64}Fe_{0.36}$)O ferropericlase based on in situ X-ray diffraction to 26.7GPa and 2173K. *Physics of the Earth and Planetary Interiors*, *151*(1–2), 163–176. https://doi.org/10.1016/j.pepi.2005.03.001

Wicks, J. K., Jackson, J. M., Sturhahn, W., & Zhang, D. (2017). Sound velocity and density of magnesiowüstites: Implications for ultralow-velocity zone topography. *Geophysical Research Letters*, *44*(5), 2148–2158. https://doi.org/10.1002/2016gl071225

Wu, Z., Justo, J. F., & Wentzcovitch, R. M. (2013). Elastic anomalies in a spin-crossover system: Ferropericlase at lower mantle conditions. *Physical Review Letters*, *110*(22), 228501. https://doi.org/10.1103/PhysRevLett.110.228501

Yang, J., Lin, J. F., Jacobsen, S. D., Seymour, N. M., Tkachev, S. N., & Prakapenka, V. B. (2016). Elasticity of ferropericlase and seismic heterogeneity in the Earth's lower mantle. *Journal of Geophysical Research: Solid Earth*, *121*(12), 8488–8500. https://doi.org/10.1002/2016jb013352

Yang, J., Tong, X., Lin, J.-F., Okuchi, T., & Tomioka, N. (2015). Elasticity of ferropericlase across the spin crossover in the Earth's lower mantle. *Scientific Reports*, *5*(1), 17188. https://doi.org/10.1038/srep17188

Yang, K., Wang, X., Zhang, J., Cheng, Y., Zhang, C., Zeng, Z., & Lin, H. (2021). Entropic broadening of the spin-crossover pressure in ferropericlase. *Physical Review B*, *103*(22), 224105. https://doi.org/10.1103/physrevb.103.224105

Yu, S., & Garnero, E. J. (2018). Ultralow velocity zone locations: A global assessment. *Geochemistry, Geophysics, Geosystems : G3*, *19*(2), 396–414. https://doi.org/10.1002/2017GC007281

Zhang, J., & Kostak, P. (2002). Thermal equation of state of magnesiowüstite ($Mg_{0.6}Fe_{0.4}$)O. *Physics of the Earth and Planetary Interiors*, *129*(3), 301–311. https://doi.org/10.1016/S0031-9201(01)00296-5

Zhuravlev, K. K., Jackson, J. M., Wolf, A. S., Wicks, J. K., Yan, J., & Clark, S. M. (2010). Isothermal compression behavior of (Mg,Fe)O using neon as a pressure medium. *Physics and Chemistry of Minerals*, *37*(7), 465–474. https://doi.org/10.1007/s00269-009-0347-6

References From the Supporting Information

Angel, R. J. (2000). Equations of state. In R. M. Hazen & R. T. Downs (Eds.), *High-temperature and high-pressure crystal chemistry* (pp. 35–60). The Mineralogical Society of America.

Coelho, A. A. (2018). TOPAS and TOPAS-academic: An optimization program integrating computer algebra and crystallographic objects written in C++. *Journal of Applied Crystallography*, *51*(1), 210–218. https://doi.org/10.1107/s1600576718000183

Dong, W., Glazyrin, K., Khandarkhaeva, S., Fedotenko, T., Bednarčík, J., Greenberg, E., et al. (2022). $Fe_{0.79}Si_{0.07}B_{0.14}$ metallic glass gaskets for high-pressure research beyond 1 Mbar. *Journal of Synchrotron Radiation*, *29*(5), 1167–1179. https://doi.org/10.1107/s1600577522007573

Finkelstein, G. J., Jackson, J. M., Sturhahn, W., Zhang, D., Alp, E. E., & Toellner, T. S. (2017). Single-crystal equations of state of magnesiowustite at high pressures. *American Mineralogist*, *102*(8), 1709–1717. https://doi.org/10.2138/am-2017-5966

Longo, M., McCammon, C. A., & Jacobsen, S. D. (2011). Microanalysis of the iron oxidation state in (Mg,Fe)O and application to the study of microscale processes. *Contributions to Mineralogy and Petrology*, *162*(6), 1249–1257. https://doi.org/10.1007/s00410-011-0649-9

McCammon, C. A. (1994). A Mössbauer milliprobe: Practical considerations. *Hyperfine Interactions*, *92*(1), 1235–1239. https://doi.org/10.1007/bf02065761

Prescher, C., McCammon, C., & Dubrovinsky, L. (2012). MossA: A program for analyzing energy-domain Mössbauer spectra from conventional and synchrotron sources. *Journal of Applied Crystallography*, *45*(2), 329–331. https://doi.org/10.1107/S0021889812004979

Prescher, C., & Prakapenka, V. B. (2015). Dioptas: A program for reduction of two-dimensional X-ray diffraction data and data exploration. *High Pressure Research*, *35*(3), 223–230. https://doi.org/10.1080/08957959.2015.1059835

Stacey, F. D., Brennan, B. J., & Irvine, R. D. (1981). Finite strain theories and comparisons with seismological data. *Geophysical Surveys*, *4*(3), 189–232. https://doi.org/10.1007/bf01449185

Takemura, K. (2021). Hydrostaticity in high pressure experiments: Some general observations and guidelines for high pressure experimenters. *High Pressure Research*, *41*(2), 155–174. https://doi.org/10.1080/08957959.2021.1903457

Wang, B. (2022). Batch peaks fitting script in Python for time-resolved XRD data analysis (v1.0.0) [Software]. *Zenodo*. https://doi.org/10.5281/zenodo.7457445